Aggregation and Reactivity of the Lithium Enolate of 2-Biphenylylcyclohexanone in Tetrahydrofuran[1]

Andrew Streitwieser* and Daniel Ze-Rong Wang

Contribution from the Department of Chemistry, University of California, Berkeley, California 94720-1460

Received February 24, 1999. Revised Manuscript Received April 19, 1999

Abstract: Deprotonation of biphenylylcyclohexanone (BPCH) with a lithium base in THF occurs preferentially at the secondary enolate position to give the unconjugated lithium enolate which is gradually converted to the more stable conjugated enolate by further proton transfer from the tertiary enolate position of the ketone. The unconjugated lithium enolate is present dominantly as the tetramer, but it is the monomer that reacts with ketone to give the conjugated enolate, LiBPCH. The conjugated enolate is present as a monomer−dimer mixture with $K_{1,2} = 4300\ M^{-1}$. The equilibrium constant changes only slightly at lower temperatures, indicating that dimerization is primarily entropy-controlled. The ion pair p*K* of LiBPCH, 12.3, is 6.0 units less than that of the corresponding cesium enolate, CsBPCH. Alkylation of LiBPCH with methyl brosylate or benzylic bromides occurs at the tertiary carbon, and $k_M \gg k_D$. These reactions are faster than those of LiPhIBP, although LiPhIBP has a higher ion pair p*K* value. The ion pair displacement reaction has a relatively low activation energy but a normal entropy of activation.

Introduction

Lithium enolates of simple ketones are known to be frequently aggregated in nonpolar solvents such as THF,[2,3] and recent attention has been directed to the possibility that aggregates are involved in controlling reaction stereochemistry.[4−6] Recent work in our laboratory has used two complementary methods for determining the stoichiometry of such aggregates and the equilibrium constants among them.[7,8] One method exploits the different UV−vis spectra of the aggregates. Singular value decomposition (SVD) analysis of a series of spectra covering a range of concentrations is used to deduce the components and their spectra. These spectra are then used to determine the concentrations of each component in the observed spectra from which the equilibrium constants are obtained. The second method makes use of *coupled equilibria*, in which the aggregation equilibrium affects an associated reaction equilibrium usually taken as that of proton transfer with a suitable indicator system. Aggregation stoichiometry and equilibrium constants are then obtained from the observed changes in the proton transfer equilibrium with concentration. We reported recently that the cesium enolate of *p*-phenylisobutyrophenone (CsPhIBP) exists as monomers, dimers, and tetramers in THF solution,[7] and that the corresponding lithium enolate (LiPhIBP) is a monomer−tetramer mixture.[8] In both cases, alkylation reactions involve dominantly the monomer. Those cases are enolates in which the enolate oxygen is not conjugated to the aromatic ring. In the present paper we compare the results to the lithium enolate of 2-(4-biphenylyl)cyclohexanone, LiBPCH, in which such conjugation is a structural feature. A companion study of the corresponding cesium enolate has been reported separately.[9]

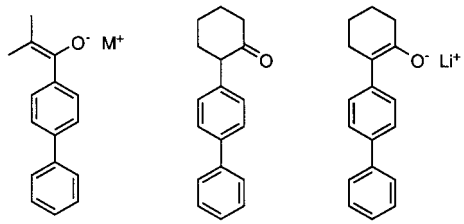

LiPhIBP (M = Li) BPCH LiBPCH

CsPhIBP (M= Cs)

Results and Discussion

Deprotonation of BPCH. The ketone was deprotonated using the conjugate lithium base of a much weaker acid, 9-lithio-9,-10,10-trimethyldihydroanthracene (LiTMDA). The lithium enolate, LiBPCH, was produced as seen by its absorbance spectrum in the UV, but the magnitude of the absorbance was much less than anticipated. If enough base was used to deprotonate to ketone completely, the resulting solutions were stable indefinitely. If insufficient base was used, however, the absorbance of LiBPCH increased gradually to the anticipated maximum. These results were interpreted as an initial kinetic proton transfer to give both the conjugated (LiBPCH) and nonconjugated (**1**) lithium enolates. The latter has no absorbance in the UV region used and is converted to the more stable conjugated enolate by reaction with ketone (Scheme 1). From the extinction coefficient of LiBPCH determined below, the initial deprotonation gave a 87:13 mixture of **1**/LiBPCH. The kinetic formation of less stable

(1) Carbon Acidity. 109. E-mail address: astreit@socrates.berkeley.edu.

(2) Seebach, D. *Angew. Chem., Int. Ed. Engl.* **1988**, *27*, 1624−1654. Heathcock, C. H. In *Comprehensive Synthetic Chemistry*; Trost, B., Ed.; Pergamon Press: New York, 1991; pp 181−238.

(3) Jackman, L. M.; Bortiatynski, J. *Adv. Carbanion Chem.* **1992**, *1*, 45−87.

(4) Williard, P. G.; Salvino, J. M. *Tetrahedron Lett.* **1985**, *26*, 3931−4.

(5) Wei, Y.; Bakthavatchalam, R. *Tetrahedron* **1993**, *49*, 2373−2390.

(6) Juaristi, E.; Beck, A. K.; Hansen, J.; Matt, T.; Mukhopadhyay, T.; Simson, M.; Seebach, D. *Synthesis* **1993**, 1271−90.

(7) Streitwieser, A.; Krom, J. A.; Kilway, K. A.; Abbotto, A. *J. Am. Chem. Soc.* **1998**, *120*, 10801−6.

(8) Abbotto, A.; Leung, S. S.-W.; Streitwieser, A.; Kilway, K. V. *J. Am. Chem. Soc.* **1998**, *120*, 10807−13.

(9) Streitwieser, A.; Wang, D. Z.-R.; Stratakis, M. *J. Org. Chem.*, in press.

10.1021/ja990593h CCC: $18.00
Published on Web 06/16/1999

Scheme 1

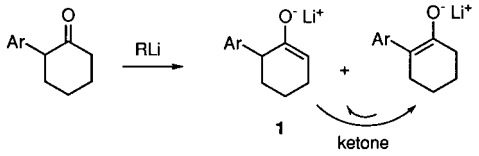

Table 1. Energies of Lithium Enolates of Phenylcyclohexanone

method	*E*(conjugated), au	*E*(unconjugated), au	ΔE, kcal mol^{-1}
HF/6-31G*	−544.350 091	−544.340 048	6.30
HF/6-31+G*	−544.362 157	−544.352 671	5.95

enolates is not new. For example, Chyall et al.[10] found kinetic base deprotonation of 3-Me-2-butanone and 2-Me-3-pentanone to give preferentially the less substituted enolate in the gas phase. Xie, Saunders, and Beutelman[11,12] have found that deprotonation of several ketones with LDA in THF at 0 °C gives predominantly the less substituted lithium enolate.

Because of conjugation with the aromatic ring, LiBPCH is more stable than **1** and dominates the equilibrium. The same observations were made in less detailed studies of the lithium enolate of 2-phenylcyclohexanone, LiPCH, and **1** (Ar = phenyl).[13] Conjugation with a phenyl group is usually estimated to be worth about 5 kcal mol^{-1}. To get a better measure, ab initio computations[14] were made on the two lithium enolates of phenylcyclohexanone with the results shown in Table 1. The corresponding optimized structures are given in Table S1 (Supporting Information). The energy difference of about 6 kcal mol^{-1} for the monomers in the gas phase corresponds to an equilibrium constant of $>10^4$. If a similar equilibrium constant applies to the THF solutions of LiPCH or LiBPCH and **1**, less than 0.01% of **1** remains at equilibrium with the conjugated enolates.

To measure the spectrum and extinction coefficient of LiBPCH, the ketone was treated successively with the base LiTMDA in a type of prolonged titration to convert the base entirely to the conjugated enolate whose concentration was taken as that of the base used. In each of several experiments the resulting solution was then successively diluted with THF to provide spectra of LiBPCH over a wide range of concentrations. The results of three runs are summarized in Table S2 (Supporting Information). The spectra showed a variation in λ_{max} from 361.5 to 382.5 nm over a concentration range of 1×10^{-3} to 2×10^{-5} M, showing that aggregates present have different spectra. When the spectra were normalized to the same maximum absorbance, they showed an isosbestic point at 371.5 nm (Figure S1, Supporting Information). The absorbance at the isosbestic point gave a useful extinction coefficient (Figure S2, Supporting Information) as well as indicated the presence in significant amounts of only two species whose spectra vary with concentration.

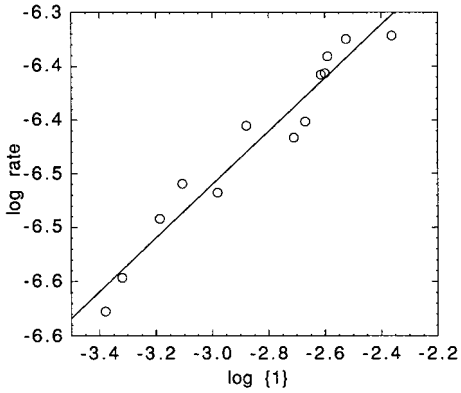

Figure 1. Log−log plot of initial rate for conversion of the unconjugated enolate, **1**, to the conjugated enolate, LiBPCH, at a constant ketone concentration and varying [**1**]. The slope of the regression line shown is 0.251 ± 0.019.

Scheme 2. Conversion of **1** to LiBPCH

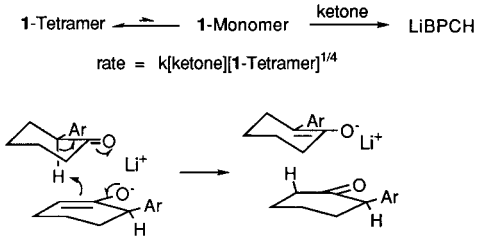

In the deprotonation of BPCH, the amount of LiTMDA used gives the total amount of enolate formed while the spectrum shows how much of this enolate is LiBPCH; the difference is taken as the corresponding **1**. Initial rates were obtained by monitoring the absorbance as a function of time. Some sample kinetic plots of this type are shown in Figure S3 (Supporting Information). The initial slopes were used for the rate analyses. The results of several kinetics measurements of the growth of LiBPCH are summarized in Table S3 (Supporting Information). At a constant concentration of the unconjugated enolate, a log−log plot of rate vs the ketone concentration has a slope of 1.07 ± 0.04, showing that the reaction is first order in ketone (Figure S4, Supporting Information). A similar plot (Figure 1) for varying the concentration of **1** at a constant ketone concentration has a slope of 0.25 ± 0.02; that is, the reaction is one-fourth order in the unconjugated enolate. We interpret this result to show that the unconjugated enolate is present dominantly as a tetramer, but it is only the small concentration of monomer present that is the actual reactant; that is, the overall reaction can be expressed as in Scheme 2. A reasonable mechanism involves direct proton transfer from ketone to enolate with both coordinated to Li^+ as shown in Scheme 2.

These results were further confirmed by reaction with trimethylchlorosilane (TMSCl). When deprotonation by LiTMDA was followed immediately by reaction with TMSCl, GC analysis of the products showed 87% of the unconjugated silyl ether. If the solution was allowed to stand for several hours in the presence of ketone, TMSCl trapping gave 97.5% of the conjugated silyl enol ether. Similarly, deprotonation by LDA followed immediately with TMSCl gave 83% of the unconjugated silyl enol ether, whereas after equilibration only the conjugated product was observed.

This result is relevant to recent interest in enantioselective protonations of lithium enolates with chiral protonating agents,[15] because it is a rare example of a demonstrated kinetic proto-

(10) Chyall, L. J.; Brickhouse, M. D.; Schnute, M. E.; Squires, R. R. *J. Am. Chem. Soc.* **1994**, *116*, 8681−90.

(11) Xie, L.; Saunders: W. H., Jr. *Z. Naturforsch.* **1989**, *44a*, 413.

(12) Beutelman, H. P.; Xie, L.; Saunders: W. H. *J. Org. Chem.* **1989**, *54*, 1703−9.

(13) Wang, D. Z.-R.; Streitwieser., A. *Can. J. Chem.* In press.

(14) Frisch, M. J.; Trucks, G. W.; Schlegel, H. B.; Gill, P. M. W.; Johnson, B. G.; Robb, M. A.; Cheeseman, J. R.; Keith, T.; Petersson, G. A.; Montgomery, J. A.; Raghavachari, K.; Al-Laham, M. A.; Zakrzewski, V. G.; Ortiz, J. V.; Foresman, J. B.; Cioslowski, J.; Stefanov, B. B.; Nanayakkara, A.; Challacombe, M.; Peng, C. Y.; Ayala, P. Y.; Chen, W.; Wong, N. W.; Andres, J. L.; Replogle, E. S.; Gomperts, R.; Martin, R. L.; Fox, D. J.; Binkley, J. S.; Defrees, D. J.; Baker, J.; Stewart, J. P.; Head-Gordon, M.; Gonzalez, C.; Pople, J. A., Gaussian, Inc., Pittsburgh, PA, 1995.

(15) Fehr, C. *Angew. Chem., Int. Ed. Engl.* **1996**, *35*, 2566−87.

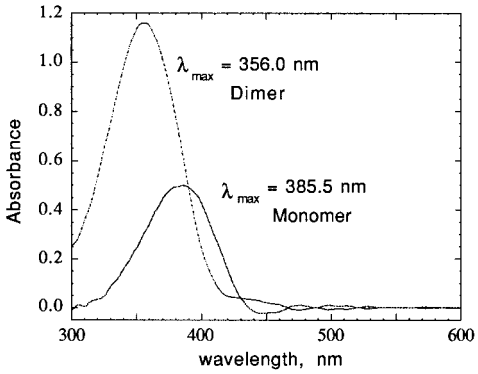

Figure 2. Spectra of monomer and dimer as given by SVD.

nation of a coordinated lithium enolate monomer in equilibrium with an aggregate.

SVD Analyis. The series of spectra were subjected to singular value decomposition as detailed previously.[16] The spectra of the monomer and dimer obtained from this analysis are shown in Figure 2. As in previous cases, the monomer has λ_{max} at longer wavelength than the aggregate and is attributed as before to a transition dipole directed from oxygen to the π-system and away from the cation. The two cations close to the enolate oxygen in the dimer electrostatically oppose this transition dipole more than the single cation in the monomer, which results in a higher energy transition.[7,8]

We have learned that the reliability of the SVD results needs to be tested.[7,8] The approach used for the present results is to compare the self-consistency of the extrapolated values for λ_{max} of monomer and dimer with those of the direct SVD. The spectra shown in Figure 2 were used to determine the composition of each spectrum used in the SVD analysis in terms of the monomer and dimer concentration; these numbers are included in Table S2 (Supporting Information), and the λ_{max} for each such spectrum was plotted against the monomer concentration. This plot is shown in Figure S5 (Supporting Information). The result is a linear correlation that extrapolates to λ_{max}(monomer) = 389 and λ_{max}(dimer) = 350, in good agreement with the spectra in Figure 6 (monomer, 385.5 nm; dimer, 356.0 nm). This consistency lends confidence to the SVD results.

The equilibrium constant for dimer formation is given by eq 1. Correspondingly, a plot of [dimer] vs [monomer]^2 gives a straight line whose slope is $K_{1,2}$. This plot is given as Figure 3;

$$2\mathrm{M} \rightleftarrows \mathrm{D} \qquad K_{1,2} = [\mathrm{D}]/[\mathrm{M}]^2 \tag{1}$$

the derived value of $K_{1,2}$ is 4.6×10^3 M^{-1}. The linearity of this plot confirms that the aggregate is the dimer. Any significant contribution from higher aggregates would cause the line to curve upward.

A limited study was made of the effect of temperature. The absorption was measured for each of nine solutions at 25 °C and at 5 °C intervals to 0 °C over a concentration range of 2.6×10^{-4} to 12×10^{-4} M. The spectra changed little over this range; the absorbance at λ_{max} increased by only 10% over this interval, but 2/3 of this change comes from contraction of the solvent;[17] that is, when corrected for the increased concentration of a given solution at reduced temperature, the extinction coefficient increased by only 3% over this 25 °C interval. With only nine solutions, SVD could not be done satisfactorily for

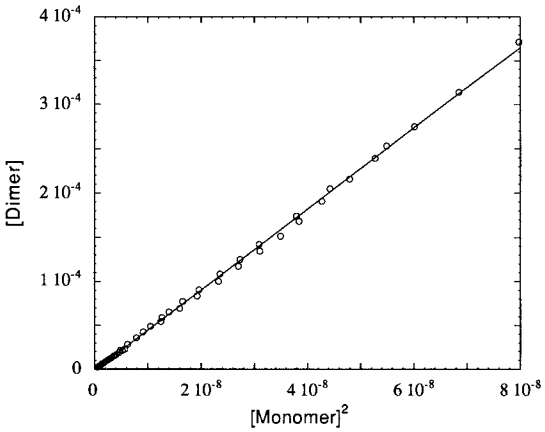

Figure 3. [Dimer] vs [monomer]^2. The equation of the line shown is $-(1.52 \pm 0.55) \times 10^{-6} + (4582 \pm 20)x$, $R^2 = 0.999$.

each temperature; however, the analysis at 20 °C did give satisfactory results. Thus, the spectra of monomer and dimer at 20 °C were used to determine the compositions of each of the spectra at all of the temperatures with adjustment for the average change in extinction coefficients at each temperature. The resulting [dimer] was plotted against [monomer]^2 to derive the $K_{1,2}$ values summarized in Table S4 (Supporting Information). These $K_{1,2}$ values show a systematic change increasing at 0 °C by 23% compared to 25 °C. A plot of $\Delta G°$ vs T (Figure S6, Supporting Information) gives $\Delta H° = -1.3$ kcal mol^{-1}. The derivation of this number is not ideal, but the small change in spectra with temperature indicates that $\Delta H°$ must have a small magnitude. Using the more accurate value of $K_{1,2} = 4300$ M^{-1} at 25 °C derived below, the corresponding $\Delta S° = 12.2 \pm 0.4$ eu. These numbers suggest that entropy dominates the equilibrium, probably by loss of solvation on dimerization, and fits with other 1:1 lithium salts in THF whose dimerization is also entropy driven.[18] These numbers are also comparable to those found for the corresponding cesium enolate, CsBPCH, $K_{1,2} = 1.9 \times 10^3$ M^{-1}, $\Delta H° = 0.7$ kcal mol^{-1}, and $\Delta S° = 17.5$ eu,[9] and for LiPCH, $K_{1,2} = 2.8 \times 10^3$ M^{-1}.[13]

Ion Pair Acidity. Comparison of spectroscopic studies with the coupled equilibria of aggregation and ion pair proton transfer has been shown to be a powerful technique for obtaining quantitative understanding of aggregation.[7,8,13,19−21] The proton transfer involves determination of the ion pair acidity as defined by eq 2 in which LiIn is a suitable indicator. The indicator needs to have an acidity comparable to that of the substrate and a spectrum sufficiently different that both can be measured. A number of indicators are now known on the lithium ion pair scale in THF.[21,22] In eq 3, {RLi} denotes the formal concentration of the lithium enolate. The indicators are lithium salts of highly delocalized carbanions that are solvent separated ion pairs

$$\mathrm{RH} + \mathrm{LiIn} \rightleftarrows \mathrm{RLi} + \mathrm{InH} \tag{2}$$

$$K_{obs} = \frac{\{\mathrm{RLi}\}[\mathrm{Inh}\}}{[\mathrm{RH}][\mathrm{LiIn}]} \tag{3}$$

(16) Krom, J. A.; Petty, J. T.; Streitwieser, A. *J. Am. Chem. Soc.* **1993**, *115*, 8024−30.

(17) *Industrial Solvents Handbook*; Flick, E. W., Ed.; Noyes Data Corp.: Park Ridge, NJ, 1985.

(18) Chabanel, M. *Pure Appl. Chem.* **1990**, *62*, 35−46.

(19) Abu-Hasanayn, F.; Stratakis, M.; Streitwieser, A. *J. Org. Chem.* **1995**, *60*, 4688−9.

(20) Abu-Hasanayn, F.; Streitwieser, A. *J. Am. Chem. Soc.* **1996**, *118*, 8136−7.

(21) Kaufman, M. J.; Gronert, S.; Streitwieser, A., Jr. *J. Am. Chem. Soc* **1988**, *110*, 2829−35.

(22) Streitwieser, A.; Wang, D. Z.; Stratakis, M.; Facchetti, A.; Gareyev, R.; Abbotto, A.; Krom, J. A.; Kilway, K. V. *Can. J. Chem.* **1998**, *76*, 765−9.

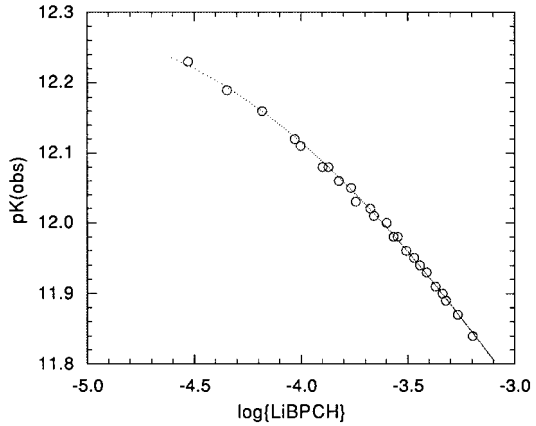

Figure 4. Observed p*K* of LiBPCH as a function of concentration. The curve shown is that calculated for $pK_o = 12.31$ (for LiBPCH monomer) and $K_{1,2} = 4300\ M^{-1}$.

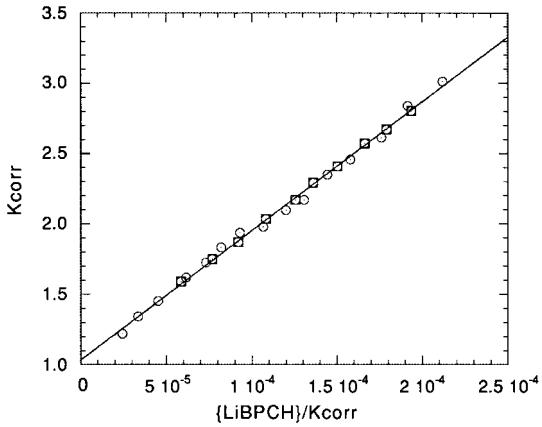

Figure 5. K_{corr} for the proton transfer equilibrium of LiBPCH with DPI vs {LiBPCH}/K_{corr}. Circles and squares are from two separate experiments. The equation of the line shown is $(1.034 \pm 0.014) + (9173 \pm 112)x$; $R^2 = 0.997$.

and have dissociation constants $K_{diss} \cong 1 \times 10^{-5}\ M^{-1}$ in THF solution.[19] The lithium enolates are contact ion pairs with much lower K_{diss}; thus, correction has to be made for dissociation of the lithiated indicators to free ions. The correction is conveniently made by eq 4.

$$K_{corr} = K_{ob}\left(1 - \frac{2}{1 - \sqrt{1 + 4[T]/K_{diss}}}\right) \qquad (4)$$

In the present case, 1,3-diphenylindene (DPI) was found to be a useful indicator. It has two maximum absorbances at 450 nm ($\epsilon = 32\,900$) and 380 nm ($\epsilon = 22\,000$) and $pK = 12.32$; 450 nm was used together with the isosbestic point of LiBPCH (371.5 nm). Mixtures were allowed to stand long enough to reach equilibrium. The resulting spectra were deconvoluted to obtain the data summarized in Table S5 (Supporting Information). A plot of p*K* vs log{LiBPCH} (Figure 4) shows the increasing observed acidity with increasing concentration associated with the increased aggregation of eq 1.

It has been shown that a plot of K_{obs} vs {enolate}/K_{obs} is a straight line for a monomer−dimer equilibrium in which the intercept gives the equilibrium acidity constant for the monomer, K_o, and the slope $= 2K_{1,2}K_o^2$.[16] Such a plot is shown in Figure 5; the derived values from the regression line are $K_o = 1.034 \pm 0.014$ ($pK_o = 12.31$) and $K_{1,2} = (4.29 \pm 0.05) \times 10^3\ M^{-1}$, a value in excellent agreement with that from the SVD analysis; the rounded value of $4300\ M^{-1}$ is used in subsequent applications. These values were used to derive the calculated dependence of the observed p*K* with concentration shown in Figure 4. The p*K* value of 12.31 is 0.4 unit lower than that of LiPCH, which has the reduced conjugation of a phenyl compared to a biphenylyl group.[13] It is 3.5 units lower than that for the lithium enolate of *p*-phenylisobutyrophenone (LiPhIBP), in which the aryl substituent is not directly conjugated with the enolate function. In accord with the generalization made earlier,[23] the more basic enolate is also more aggregated. This generalization is also consistent with the behavior of the two lithium enolate isomers in the present study: the less conjugated **1** is also more basic and more aggregated.

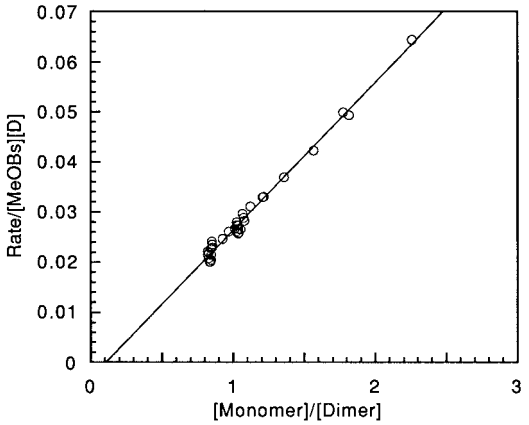

Figure 6. Rate/[MeOBs][dimer] vs [monomer]/[dimer]. The intercept gives $k_D = -0.0031 \pm 0.0006$; the slope gives $k_M = 0.0295 \pm 0.0005$; $R^2 = 0.989$.

Note that in this work there is no direct evidence of mixed aggregates between **1** and LiBPCH. The kinetic studies with **1** discussed above indicate a homotetramer, but these studies involved initial rates under conditions where [**1**] ≫ [LiBPCH]. Nevertheless, if there were a substantial tendency toward mixed aggregate formation, the kinetics would have shown larger than one-fourth-order dependence on {**1**}. Since **1** is predominantly a tetramer and LiBPCH a dimer, it seems likely that **1** prefers to aggregate with itself (being effectively more basic), thus leaving LiBPCH to also self-aggregate. This suggestion that the tendency to form mixed aggregates might depend on the homoaggregation of the components seems worthy of subsequent experimental test. In any event, at equilibrium, the amount of **1** present is too small for any detectable effect.

Alkylation Reactions. With the aggregation information in hand, one can now study the alkylation kinetics of LiBPCH to determine the relative reactivities of monomer and dimer. Alkylation reactions were carried out with methyl brosylate (MeOBs) and several benzylic bromides. To measure the kinetics, the ketone was first deprotonated with LiTMDA to its end point, and a small additional amount of ketone was added. The mixture was allowed to stand overnight to convert the enolate mixture completely to LiBPCH, and the desired alkylating agent was then added. The spectra of these solutions were monitored at the isosbestic point of LiBPCH (371.5 nm) for determination of the initial rates. The results for 36 kinetic runs with MeOBs are shown in Table S6 (Supporting Information). One series of runs was at constant {LiBPCH} and varying [MeOBs]; a log−log plot of rate vs [MeOBs] gives a straight line (Figure S7, Supporting Information) with a slope of 0.98, indicating that the reaction is, as expected, first order in the alkylating agent. Although some information can be obtained

(23) Ciula, J. C.; Streitwieser, A. *J. Org. Chem.* **1992**, *57*, 431−432; correction p 6686.

Scheme 3

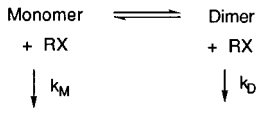

$$\text{Rate} = k_M[\text{Monomer}][RX] + k_D[\text{Dimer}][RX] \quad (5)$$

$$\text{Rate}/[RX][\text{Dimer}] = k_M[\text{Monomer}]/[\text{Dimer}] + k_D \quad (6)$$

from similar plots at constant [MeOBs] and varying {LiBPCH}, another way to obtain kinetic information in terms of LiBPCH is by use of the analysis in Scheme 3.[20] Equation 6 has a linear form in which the slope gives k_M and the intercept is k_D. The results of such an analysis for the 36 MeOBs runs in Table S6 are shown in Figure 6. The second-order rate constant for the dimer is negative, but since negative rate constants are not physically meaningful, k_2(dimer) is clearly zero within experimental error and the negative intercept gives a measure of the experimental uncertainties. The reactivity of the monomer is clearly much greater than that of the dimer. Another check is to compare the rate divided by [MeOBs] with [monomer] as shown in Figure S8 (Supporting Information); the result is a linear relation corresponding to $k_2 = 0.026$ M^{-1} s^{-1} in good agreement with the result from eq 6 ($k_2 = 0.030$ M^{-1} s^{-1}). There is no evidence of upward curvature that would indicate a significant role for reaction with dimer. In applying eq 6, it is best to keep the ratio [monomer]/[dimer] as low as possible; that is, the concentrations of {LiBPCH} should be as high as feasible. There are clear limitations in how high we could go using UV−vis methods, but in general, values of [monomer]/[dimer] > 3 were not used.

The product of the MeOBs reaction is entirely that of C-alkylation; this result contrasts with the reaction of LiPhIBP with methyl tosylate, in which much O-alkylation was found.[8] The difference is probably associated with the lower basicity of LiBPCH.

The runs with the benzylic bromides were analyzed in the same way. The results for benzyl bromide and *o*-chloro-, *m*-chloro-, and *o*-methylbenzyl bromides are summarized in Table S7 (Supporting Information). In all of the plots following eq 6 the rate constants for dimer were close to zero. The rate constants for the monomer were similar to those obtained by direct comparison of the rate with monomer concentration (Figures S9−S12, Supporting Information); the latter values of k_2(monomer) are considered to be more accurate. These rate constants are summarized in Table 2. None of the direct plots of rate vs [monomer] show any upward curvature indicative of significant reaction of dimer. From these results, it is clear that $k_M \gg k_D$, but the experimental errors place only a lower limit on the ratio k_M/k_D of 1−2 orders of magnitude. A ratio of 2 orders of magnitude means that under synthesis conditions where {LiBPCH} is on the order of a few tenths molar alkylation still occurs dominantly through the monomer.

The reaction of free ions from dissociation of the lithium enolate as in eq 7 would give rise to half-order kinetics; however, triple ions as in eq 8 would enter kinetically as the

$$RO^-Li^+ \rightleftarrows RO^- + Li^+ \quad (7)$$

$$(RO^-Li^+)_2 \rightleftarrows (RO^-)_2Li^+ + Li^+ \quad (8)$$

monomer in the absence of added lithium cation. To test this possibility, kinetic measurements were made on the reaction of *m*-chlorobenzyl bromide in the presence of lithium tetraphenylborate. These data are summarized in Table S8 (Supporting Information). Rate constants were extracted from the initial rates by eq 6 and by direct comparison with [monomer] and are listed in Table 3 and shown in Figure S13 (Supporting Information). At concentrations of $LiBPh_4$ below 0.001 M, there is clearly no significant effect; thus, involvement of free ions or triple ions can be ruled out. At high concentrations on the order of 0.01 M, there is evidence for some effect, but since the $K_{1,2}$ used was that in the absence of $LiBPh_4$, it is not possible to tell whether the effect is on this equilibrium or on the reaction rates.

The reproducibility of the reactions and the substituent effects are consistent with these alkylations being ion pair S_N2 reactions. An important and unexpected result of these ion pair S_N2 reactions concerns the relative rates of LiBPCH monomer compared to LiPhIBP monomer toward the same benzylic halides. LiBPCH is less basic than LiPhIBP (by 3.5 p*K* units; vide supra), yet it is more reactive toward benzylic bromides! The rate ratio is 6.6 for benzyl bromide and 5.7 for *m*-chlorobenzyl bromide; the ratios are lower for the ortho-substituted benzyl bromides in which steric hindrance might play some role.[8] The explanation is probably that lithium cation is electrostatically more strongly bound to the more basic oxygen of LiPhIBP and requires more energy to become a looser cation in the reaction transition state. This explanation finds support in the relative p*K* values; CsPhIBP has a p*K* 9.3 units higher than that of CsBPCH compared to a difference of only 3.5 units for the lithium enolates.[7,9] Moreover, in line with the relative basicities of the cesium enolates, CsPhIBP monomer is more reactive (by about an order of magnitude) toward methyl tosylate and *p-tert*-butylbenzyl chloride than is CsBPCH, the opposite reactivity order of the lithium enolates.

Rates of reaction of *m*-chlorobenzyl bromide were carried out at 5 °C intervals to 0 °C. The initial changes in absorbance with time were converted to rates of reaction of LiBPCH using the extinction coefficients at each temperature as measured above. The concentrations of the bromide were about 0.008 M, and the concentrations of LiBPCH monomer were determined from $K_{1,2}$ at room temperature (4300 M^{-1}) corrected for the small temperature coefficient derived above). Plots of the rate vs [monomer][RBr] are shown in Figure S14 (Supporting Information), and the derived rate constants are summarized in Table 4. The errors shown are just those of the fittings in Figure S13. Because of uncertainties in the $K_{1,2}$ values, the errors are undoubtedly higher. A plot of ln *k* vs 1/*T* is shown in Figure S15 (Supporting Information) and corresponds to an activation energy $\Delta E^* = 10.2 \pm 0.9$ kcal mol^{-1}, $\log A = 7.65 \pm 0.66$, or, in terms of absolute rate theory, $\Delta H^‡ = 9.6 \pm 0.9$ kcal mol^{-1}, $\Delta S^‡ = -25.5 \pm 2.2$ eu. The entropy term is normal for a bimolecular reaction but suggests that the loss of 3 degrees of translational freedom of one reactant is not compensated by loss of solvation of lithium cation; that is, the lithium cation in the transition state is about as solvated as it is in LiBPCH monomer.

Conclusion

Deprotonation of 2-(*p*-biphenylyl)cyclohexanone with a lithium base in THF occurs preferentially at the secondary enolate position to give the unconjugated lithium enolate which is gradually converted to the more stable conjugated enolate by further proton transfer from the tertiary enolate position of the ketone. The unconjugated lithium enolate is present dominantly as the tetramer, but it is the monomer that reacts with ketone to give the conjugated enolate, LiBPCH. The conjugated enolate is present as a monomer−dimer mixture with $K_{1,2} = 4.3 \times 10^3$ M^{-1}. The equilibrium constant changes only slightly at lower temperatures, indicating that dimerization is primarily entropy-

Table 2. Second-Order Rate Constants (M^{-1} s^{-1}) for Alkylation of LiBPCH Monomer and Dimer

RX	$k_{2(\text{dimer})}$[a]	$k_{2(\text{monomer})}$[a]	$k_{2(\text{monomer})}$[b]
methyl brosylate	$-(3.1 \pm 0.6) \times 10^{-3}$	$(2.95 \pm 0.05) \times 10^{-2}$	$(2.63 \pm 0.02) \times 10^{-2}$
benzyl bromide	0.070 ± 0.035	0.717 ± 0.024	0.779 ± 0.010
m-chlorobenzyl bromide	0.014 ± 0.027	1.45 ± 0.02	1.47 ± 0.01
o-chlorobenzyl bromide	0.033 ± 0.037	0.501 ± 0.024	0.497 ± 0.017
o-methylbenzyl bromide	-0.006 ± 0.039	0.664 ± 0.023	0.655 ± 0.007

[a] From eq 6. [b] From direct plot of rate/[RX] vs [monomer].

Table 3. Reaction with *m*-Chlorobenzyl Bromide with Added $LiBPh_4$

$[LiBPh_4]$, M	$k_{2(\text{dimer})}$[a]	$k_{2(\text{monomer})}$[a]	$k_{2(\text{monomer})}$[b]
0	0.014 ± 0.027	1.45 ± 0.02	1.47 ± 0.01
4.9×10^{-5}	0.27 ± 0.09	1.48 ± 0.07	1.74 ± 0.03
9.7×10^{-5}	0.07 ± 0.09	1.55 ± 0.06	1.65 ± 0.04
5.2×10^{-4}	0.22 ± 0.09	1.42 ± 0.06	1.65 ± 0.04
9.1×10^{-3}	0.37 ± 0.09	1.71 ± 0.06	2.16 ± 0.09

[a] From eq 6. [b] From direct plot of rate/[RX] vs [monomer].

Table 4. Reaction of *m*-Chlorobenzyl Bromide with LiBPCH Monomer at Various Temperatures

temp, °C	k_2, M^{-1} s^{-1}	temp, °C	k_2, M^{-1} s^{-1}
0	0.36 ± 0.01	15	0.79 ± 0.03
5	0.39 ± 0.01	20	1.40 ± 0.08
10	0.63 ± 0.01	25	1.47 ± 0.01[a]

[a] From Table 9.

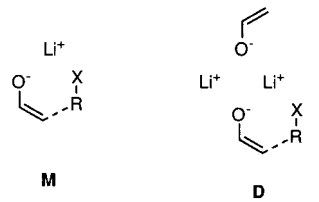

Figure 7. Suggested transition structures for alkylation reactions of monomer and dimer lithium enolates rationalizing the greater reactivity of monomer.

controlled, probably by loss of solvent molecules around lithium cation on dimerization.

The ion pair p*K* of LiBPCH, 12.3, is 6.0 units less than that of the corresponding cesium enolate, CsBPCH, and documents the strength of the electrostatic bond between the small lithium cation and the enolate oxygen anion. Alkylation of LiBPCH with methyl brosylate or benzylic bromides occurs at the tertiary carbon, and $k_M \gg k_D$. These reactions are faster than those of LiPhIBP, although LiPhIBP has a higher ion pair p*K* value. The ion pair displacement reaction has a relatively low activation energy but a normal entropy of activation consistent with a transition state that is as solvated as in the enolate monomer and with the additional coordination implied in the six-membered transition structures suggested earlier.[7] This transition structure helps rationalize the greater reactivity of the enolate monomer as shown in Figure 7. In the dimer, the enolate oxygen is coordinated to a second lithium cation and is therefore electrostatically less nucleophilic. Similarly, the lithium cation is coordinated to a second oxide ion and is electrostatically less able to attract the leaving halide or sulfonate anion.

In these transition structures the bond angle at the central carbon is significantly less than the ideal 180° considered optimal by numerous computational studies over the years[24] and several experiments.[25] These studies, however, apply generally to reactions of nucleophiles that are anions. In ion pair S_N2 reactions, the transition structures generally have bond angles less than 180°, although reaction barriers are lower with larger angles.[26,27] The transition structure for reaction of lithium vinyloxide with methyl bromide, for example, has a reaction bond angle of 143° and a relatively low barrier.[28] Thus, for ion pair S_N2 reactions, transition structures such as those in Figure 7 are probably quite reasonable.

Experimental Section

2-(*p*-Biphenylyl)cyclohexanone and the indicators were available from previous studies. The alkylating agents are commercial materials purified by distillation or crystallization before use. The general techniques have also been discussed in previous papers.[8,13,16] In the present work, however, the involvement of the nonconjugated enolate required additional precautions. To determine the extinction coefficient of LiBPCH, the following technique is an example: To a 1 mm UV quartz cell was added 0.667 g of THF, and the spectrum of THF was taken as a baseline; then 0.187 mg of BPCH was weighed into the cell, followed by 14.0 μL of the LiTMDA base solution, to deprotonate the ketone, giving a total lithium enolate concentration of 9.68×10^{-4} M. To another UV cell were added 0.558 g of THF and 1.040 mg of BPCH ([BPCH] = 6.35×10^{-4} M). The BPCH solution was added to the enolate solution in portions to quench the excess base LiTMDA (monitored by its absorption spectrum). The absorption of LiBPCH at 366 nm gradually increased. About 2 μL of BPCH solution was added in excess (2% excess), and the solution was kept for 2 days to ensure complete conversion of unconjugated to conjugated enolate before measurement of the extinction coefficient of LiBPCH.

Reaction of Enolate with TMSCl. The ketone was deprotonated with LiTMDA, and TMSCl was added immediately. The products were analyzed by GC to give relative areas of 3.54 for the unconjugated silyl ether (shorter retention time) and 0.55 for the conjugated ether. When the enolate solution was allowed to stand in the presence of a small amount of BPCH for 8 h before addition of the TMSCl, the relative areas of unconjugated/conjugated ether were 0.84:32.3. For deprotonation with LDA the kinetic products gave relative areas of 75.4 unconjugated ether and 8.86 and 7.12 of two other products. The thermodynamic mixture gave only a single silyl ether product.

1-(Trimethylsilyloxy)-6-(*p*-biphenylyl)cyclohexene. ^{1}H NMR ($CDCl_3$, 400 MHz, δ ppm): 7.63, dd, $J_1 = 7.6$ Hz, $J_2 = 0.8$ Hz, 2H; 7.56, dd, $J_1 = 8.0$ Hz, $J_2 = 2.0$ Hz, 2H; 7.45, t, $J = 8.0$ Hz, 2H; 7.32−7.37, multi, 3H; 5.13, t, $J = 4.0$ Hz, 1H; 3.44, t, $J = 8.0$ Hz, 1H; 2.15−2.25, multi, 2H; 2.04−2.12, multi, 1H; 1.74−1.83, multi, 1H; d 1.58−1.68, multi, 1H; 1.51−1.57, multi, 1H; 0.10, s, 9H. ^{13}C NMR ($CDCl_3$, 400 MHz, ppm): 150.69, 143.48, 141.19, 138.78, 128.80, 128.65, 126.98, 126.91, 126.69, 105.97, 45.616, 32.723, 24.129, 19.312, 0.254. HRMS: 322.1746 (found), 322.1753 (calculated). MS (EI) (*m*/*z*, rel intens): 322 (M^+, 100.0), 323 ($M + 1^+$, 27.8), 307 ($M^+ - Me$, 8.9), 293 ($M^+ - Me - CH_2$, 6.3), 250 ($M^+ + 1 - SiMe3$, 6.1), 167 (7.25), 155 (3.0).

(24) See the summary in Shaik, S. S.; Schlegel, H. B.; Wolfe, S. *Theoretical Aspects of Physical Organic Chemistry. The S_N2 Mechanism*; John Wiley & Sons: New York, 1992.

(25) Examples are the endocyclic restriction test applied to S_N2 reactions by Tenud et al. (Tenud, L.; Farooq, S.; Seibl, J. Eschenmoser, A. *Helv. Chim. Acta* **1970**, *53*, 2059−69) and summarized by Beak (Beak, P. *Acc. Chem. Res.* **1992**, *25*, 215−222).

(26) Harder, S.; Streitwieser, A.; Petty, J. T.; Schleyer, P. v. R. *J. Am. Chem. Soc.* **1995**, *117*, 3253−9.

(27) Choy, G. S.-C.; Abu-Hasanayn, F.; Streitwieser, A. *J. Am. Chem. Soc.* **1997**, *119*, 5013−9.

(28) Choy, G. S.-C. Results to be published.

1-(Trimethylsilyloxy)-2-(*p*-biphenylyl)cyclohexene. ^{1}H NMR ($CDCl_3$, 400 MHz, ppm): δ 7.65, dt, $J_1 = 7.2$ Hz, $J_2 = 1.2$ Hz, 2H; 7.55−7.57, multi, 2H; 7.49−7.51, multi, 2H; 7.43−7.47, td, $J_1 = 7.6$ Hz, $J_2 = 1.2$ Hz, 2H; 7.34, tt, $J_1 = 7.2$ Hz, $J_2 = 1.2$ Hz, ^{1}H; 2.44, t, $J = 6.0$ Hz, 2H; 2.23, t, $J = 6.0$ Hz, 2H; 1.71−1.82, multi, 4H; 0.03, s, 9H. ^{13}C NMR ($CDCl_3$, 400 MHz, ppm): 146.07, 141.14, 140.36, 138.05, 128.78, 128.64, 126.85, 126.17, 115.63, 31.136, 29.199, 23.385, 19.290, 0.549.

For the p*K* measurements with known amounts of 1,3-diphenylindene (DPI) the mixtures were allowed to stand until equilibrium was reached; the spectrum of the mixture was deconvoluted to obtain the concentrations of LiBPCH and LiDPI.

Acknowledgment. This research was supported in part by NIH Grant GM30369. We also thank Dr. Manolis Stratakis for preliminary experiments.

Supporting Information Available: Tables of ab initio calculation results, spectral data, ion pair acidities, and alkylation kinetics (Tables S1−S8 and Figures S1−S15 (PDF). This material is available free of charge via the Internet at http://pubs.acs.org.

JA990593H